Spatiotemporal Single-Photon Airy Bullets

Jianmin Wang,[1,2] Ying Zuo,[1,2] Xingchang Wang,[1,2] Demetrios N. Christodoulides,[4]
Georgios A. Siviloglou,[1,2,*] and J. F. Chen[1,2,3,†]

[1]*Shenzhen Institute for Quantum Science and Engineering, Southern University of Science and Technology, Shenzhen, 518055, China*
[2]*Shenzhen International Quantum Academy, Shenzhen, 518048, China*
[3]*Department of Physics, Southern University of Science and Technology, Shenzhen, 518055, China*
[4]*Ming Hsieh Department of Electrical and Computer Engineering, University of Southern California, Los Angeles, 90089, USA*

Uninhibited control of the complex spatiotemporal quantum wave function of a single photon has so far remained elusive even though it can dramatically increase the encoding flexibility and thus the information capacity of a photonic quantum link. By fusing temporal waveform generation in an atomic ensemble and spatial single-photon shaping, we hereby demonstrate for the first time complete spatiotemporal control of a propagation invariant $(2 + 1)$D Airy single-photon optical bullet. These correlated photons are not only self-accelerating and impervious to spreading as their classical counterparts, but can be concealed and revealed in the presence of strong classical stray light.

In the quest for boosting the information capacity and security of tomorrow's quantum communication links, considerable effort has been made toward harnessing the properties of entangled flying photons within their available degrees of freedom, e.g., frequency, polarization, and orbital angular momentum, to mention a few [1–6]. Remarkably, the spatial and temporal degrees of freedom—perhaps the most archetypical ones—have not been simultaneously exploited in generating robust propagation invariant information-carrying wave packets [7].

One of the most prominent members of such nonspreading wavefronts is that associated with self-bending optical fields: the Airy beam. Unlike any other class of non-diffracting waves that relies on conical superposition [8], these intriguing self-healing waves tend to freely propagate with minimal expansion while their intensity features move in a self-similar manner along curved trajectories. After their experimental observation, Airy beams [9] have found numerous applications in optical and electron microscopies [10–12], plasma generation [13,14], ultrafast optics [15], and hot atomic vapors [16], as well as in microparticle manipulation [17,18]. Even though their extraordinary attributes have been extensively investigated within the realm of classical optics [19], the same is not true for their quantum counterparts.

In recent years, nonclassical Airy beams have been demonstrated through spontaneous parametric down-conversion in nonlinear crystals [20–22] in the spatial but not in the temporal domain. Evidently, merging Airy quantum wave packets in space and time can be used to synthesize spatiotemporal photon bullets [23] that can traverse homogeneous space spatially undistorted while also being impervious to temporal dispersion. Generating a nonclassical

photon bullet is by no means a straightforward task given that the photon statistics always reflect the quantum or classical nature of the optical source, even when dimmed at extremely low levels. Realizing optical bullets [9,15] in quantum settings will require altogether new strategies for single-photon manipulation.

In this work, we demonstrate for the first time in the quantum realm spatiotemporal Airy wave packets. This is achieved using heralded single photons with subnatural linewidth and thus long coherence time, produced in an atomic medium by transferring the spatial degree of freedom into the temporal domain (space-time morphing) [24]. We show that these single-photon wave packets can be retrieved even when embedded in noisy environments. Our methodology allows one to synthesize in a robust and versatile manner arbitrary quantum nonspreading spatiotemporal light bullets and in this respect could have ramifications in a broad range of applications such as quantum imaging, long-distance quantum communications, and multidimensional information encoding.

To generate pairs of entangled photons we use an elongated cloud of Doppler cooled rubidium atoms, as shown in Fig. 1(a). The atoms are prepared to the lowest hyperfine manifold $|1\rangle$ in a two-dimensional magneto-optical trap (MOT). After MOT loading, the atoms are released and a 1.0 ms of biphoton generation via spontaneous four-wave mixing (SFWM) takes place. A pump ω_p and a control beam ω_c generate entangled Stokes ω_S and anti-Stokes photons ω_{AS}, as shown in the four-level system of Fig. 1(b). The emission of the generated photons by the opposite ends of the cloud is determined by the phase matching condition along the elongated atomic trap [24]. The transverse spatial profile of the pump beam is shaped
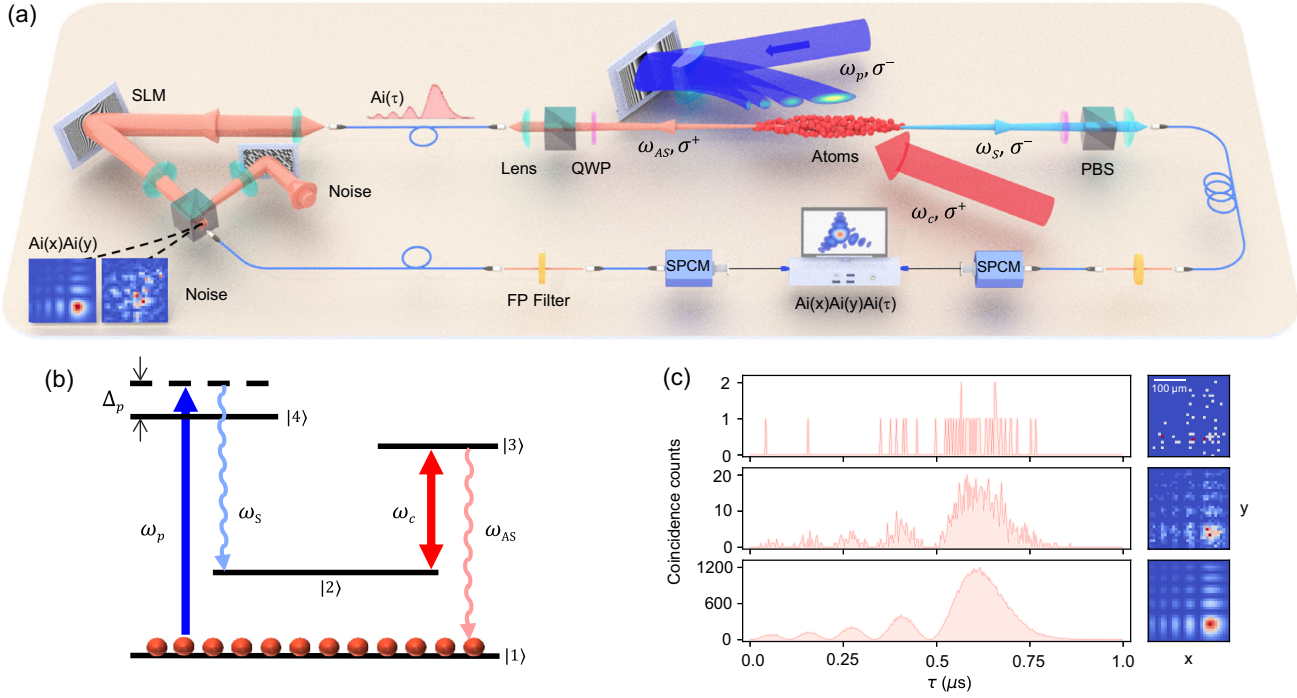
FIG. 1. Experimental scheme for the observation of spatiotemporal Airy biphotons. (a) Optical setup. Two classical circularly polarized (σ), counterpropagating beams with frequencies ω_p (Airy) and ω_c (Gaussian) generate circularly polarized Stokes, ω_S, and anti-Stokes, ω_{AS}, entangled photons via spontaneous four-wave mixing. A space-to-time mapping generates nonclassical temporal Airy biphotons Ai(τ). The ω_{AS} photons are subsequently shaped into a nondiffracting Airy wave packet to form a three-dimensional spatiotemporal photon, Ai(x)Ai(y)Ai(τ). Single-photon counting modules (SPCM) register the photons that have been filtered by Fabry-Pérot (FP) cavities. A classical noise pattern is superimposed for correlated photon concealing. (b) Double-Λ configuration for spontaneous four-wave mixing. The 780 nm 1D-Airy pump beam, ω_p, has a detuning of $\Delta_p = 120$ MHz, while the 795 nm coupling beam, ω_c, is on resonance. The twin photons ω_S (780 nm) and ω_{AS} (795 nm) are spontaneously emitted. (c) Simulated formation of spatiotemporal quantum Airy wave packets as the photon number is increased. The temporal (left) and the spatial (right) wave packets emerge simultaneously.

into a one-dimensional Airy beam by a spatial light modulator (SLM), as shown in Fig. 1(a). The Stokes photons act as a trigger to herald the slow anti-Stokes photons which are delayed by τ. Subsequently, the time-modulated anti-Stokes photons are spatially manipulated by an SLM.

A longitudinally uniform coupling beam is combined with a far-detuned and weak pump beam. The photon pairs are simultaneously created via SFWM from single atoms. Since the Stokes photons are far-detuned from the atomic resonance, they fly throughout the cloud with the speed of light. Conversely, the anti-Stokes photons are on-resonance, and experience the slowing effect stemming from electromagnetically induced transparency (EIT). When the EIT window is well within the third-order nonlinear susceptibility spectrum $\chi^{(3)}(\omega)$, the biphoton wave function $\psi(\tau)$ is [24,25]:

$$\psi(\tau) \propto \chi^{(3)}(0) E_c E_p V_g f_p \left(\frac{L}{2} - V_g \tau \right), \qquad (1)$$

where V_g, is the group velocity of the anti-Stokes photons with a group delay $\tau_g = L/V_g = 2\gamma_{13} d/|\Omega_c|^2$ in an

L-long cold atomic ensemble with a natural linewidth γ_{13} for the transition $|1\rangle \to |3\rangle$. In this case the optical depth is d, and Ω_c is the Rabi frequency of the coupling beam. Meanwhile E_p and E_c represent the electric field amplitudes for the pump and the coupling beam while $f_p(z)$ expresses the z dependence of the pump, i.e., $\Omega_p(z) = \Omega_p f_p(z)$, with $f_p(z)$ being normalized as $\int_{-L/2}^{L/2} |f_p(z)|^2 dz/L = 1$. Specifically, for an Airy-shaped pump $f_p(z)$ is proportional to Ai(z/z_0) exp(az/z_0), with z_0 being a length scale and a a containment constant.

The physical mechanism determining the space-to-time mapping of the pump light into the desired waveform of the biphotons is elucidated in Eq. (1). It acts as a spatial multiplexing scheme controlled by the pump beam, and it is fundamentally different from the direct—but lossy—temporal reshaping, by electro-optic modulation [26].

Shaping the spatial wave function of the generated Airy biphotons can conveniently rely on methods from linear classical optics, and hence, the $(2+1)$D biphoton source reported here can be exploited for generating a number of nonclassical spatiotemporal wave packets.
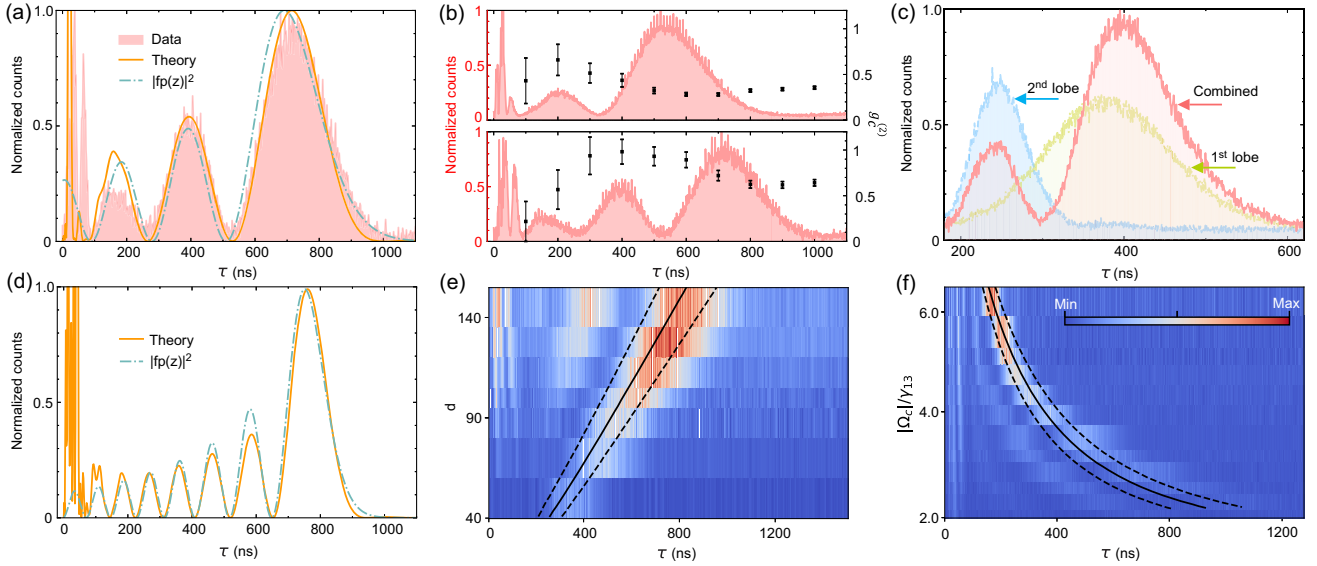
FIG. 2. Observation of temporal Airy biphotons. (a) Temporal Airy biphoton. Normalized counts of the observed biphotons (shaded pink), numerically predicted waveform (orange solid line) for $d = 150$ and $\Omega_c = 2\pi \times 10$ MHz, and analytical prediction, from Eq. (1), (dash dotted green line) for a pump having a beam profile $f_p(z) = \mathrm{Ai}(z/z_0) \exp(az/z_0)$, with $z_0 = 18.7$ mm, and $a \approx 0.1$. (b) (top) Two- and (bottom) three-lobe Airy waveforms (shaded pink) and their corresponding self-correlations, $g_c^{(2)}(\tau)$ (black squares). The biphoton generation rate for the two- and three-lobe waveforms during the SFWM is 470 s^{-1} and 374 s^{-1}. The error bars are calculated from the one standard deviation of the photon counts. (c) Locally probing the biphoton phase. Observed normalized counts when the Airy pump is imposed as a whole (shaded pink), with only the first lobe (shaded green), and only the second lobe (shaded blue). (d) Simulated (dash dotted green line), and analytical (orange solid line) Airy waveforms for high optical depths ($d = 500$). Experimentally obtained (e) temporal waveform density $|\psi(\tau)|^2$ as a function of d and fixed $\Omega_c = 2\pi \times 10$ MHz, and (f) temporal waveform as a function of the normalized coupling Rabi frequency $|\Omega_c|/\gamma_{13}$ for $d = 150$. The curves overlaid on the experimental data highlight the maximum (solid) and the half-maximum as determined by numerical simulations. The same color map is used throughout the Letter.

A three-dimensional space-time Airy wave packet has the separable form:

$$|\Psi_{xy\tau}\rangle_{z=0} = \prod_{s=x,y,\tau} \mathrm{Ai}(s/s_0) \exp(a_s s), \qquad (2)$$

where $s_0 = x_0, y_0$, and τ_0 are the spatial and temporal widths of the single-photon Airy wave function, while the a_s for $s = x, y, \tau$ are the corresponding exponential decay parameters. This nonclassical photon wave function inherits the properties of the Airy wave packet [9,19], such as nondiffraction and transversal self-bending for the spatial mode. Importantly, it also exhibits nondispersion and longitudinal acceleration for the temporal component, and self-healing as was demonstrated in [27], and only recently in the quantum realm [22]. Figure 1(c) conceptually illustrates the photon-by-photon formation of nonclassical spatiotemporal Airy wave packets.

To generate temporal Airy biphotons, we use a one-dimensional classical Airy-shaped pump, by Fourier transforming a wide Gaussian beam on which we have imprinted a cubic phase by an SLM. The characteristic Airy shape is clearly observed, Fig. 2(a), in excellent agreement with the numerical simulations [28]. In addition, our results conform with the analytical predictions, directly

from Eq. (1), for a medium with optical depth of 150 and a peak Rabi frequency for the coupling beam of $\Omega_c = 2\pi \times 10$ MHz. We note that in the first 30 ns we observe a precursor pulse [29].

To probe the nonclassical features of the generated Airy photons, we measure by Hanbury Brown–Twiss interference the photon self-correlation, $g_c^{(2)}$, for two different pump shapes, as shown in Fig. 2(b). In both cases we measure $g_c^{(2)} < 1$, thus verifying their nonclassical nature [28]. The experiments of Fig. 2(c), reveal the spatial origin of the temporal modulation of the biphotons and provide additional evidence on the manipulation of their complex (amplitude and phase) waveform. A π phase difference leads to zeroing of the wave function amplitude, approximately at the location where the first and the second lobe would be equal in isolation. As displayed in Fig. 2(d), increasing the atomic density [30] can lead to an even denser time binning.

To establish the versatility of the implemented method, we have engineered the temporal biphoton shape by varying d and Ω_c. The respective experimental results are shown in Figs. 2(e) and 2(f). In Fig. 2(e), when the atomic density is increased a pronounced Airy waveform emerges. In Fig. 2(f), it is evident that coupling power can quadratically reduce the group velocity of the photons and
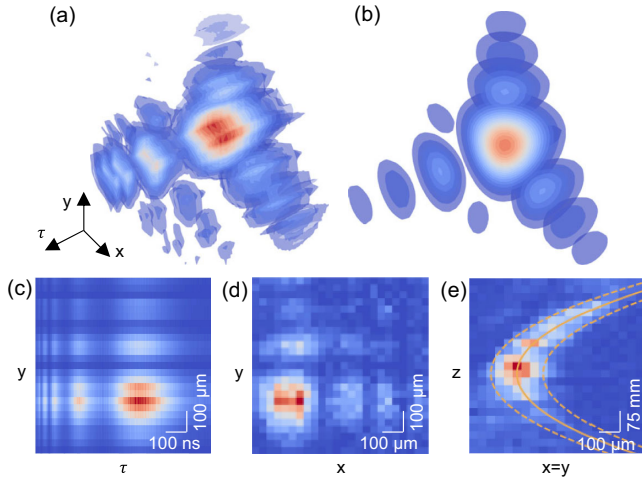
FIG. 3. A three-dimensional spatiotemporal Airy photon. Isosurface of (a) the experimentally observed $|\psi_{xy\tau}|^2$ of the Airy biphotons, and (b) the corresponding theoretical wave packets. The isosurfaces range from 0.1 to 1.0. The vector lengths represent x, y, and τ scales of 100 μm, 100 μm, and 200 ns respectively. A projection of the photon probability density (c) for the temporal τ and spatial y distribution along the x axis, and (d) for the two-dimensional spatial x, y distribution along the time axis τ. (e) Observation of the z propagation of the spatially self-bending nonclassical Airy photons along the diagonal ($x = y$). The theoretically expected parabolic trajectories (solid for the maximum and dashed for the half-maximum) are overlaid.

proportionally shrink their temporal width. Additional theoretical results are presented in [28].

In Figs. 3(a) and 3(b) the experimentally obtained spatiotemporal Airy photons are presented along with the corresponding theoretical ones. We note that this is the first realization of a single-photon nonspreading optical bullet in the quantum realm. These $(2+1)$D Airy wave packets have been observed in the classical regime of extreme nonlinear optics where the photons per pulse can exceed 10^{14} [14]. A complementary way of generating quantum Airy optical bullets without utilizing the slow light effect as is in our work would require combining the techniques reported in [4,15]. A noteworthy difference is that for the atomic systems the spectral brightness is particularly high because of the sub-MHz EIT widths.

The projection of the spatiotemporal Airy photons on the temporal τ and spatial dimension y, as seen from the x direction, is shown in Fig. 3(c), while the complementary spatial photon shape is shown in Fig. 3(d). The self-bending propagation of the single photons is shown in Fig. 3(e), and is observed by introducing an additional quadratic phase, which is equivalent to the phase term appearing in Fresnel diffraction [28]. Our method enables us to freely synthesize nonclassical spatiotemporal wave packets.

The nondiffracting and accelerating properties of the spatial Airy beams can now be complemented by their quantum realization. We have taken advantage of photon
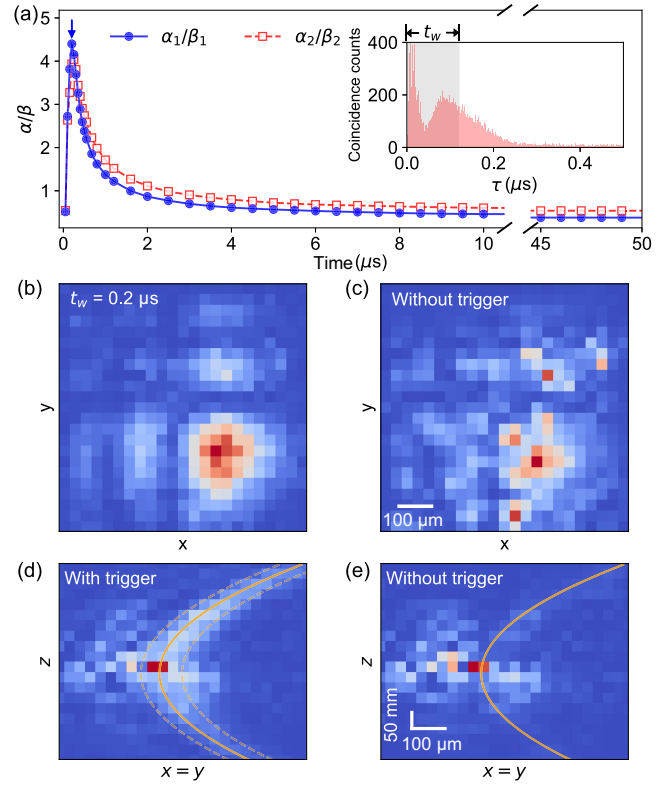

FIG. 4. Concealing correlated nondiffracting photons in classical light noise. (a) Airy to noise ratio α/β as a function of time window t_w. Blue and red lines show two measurements with different classical noise powers. The inset depicts a typical biphoton waveform for a Gaussian pump. The blue arrow corresponds to image (b) for $t_w = 0.2$ μs of collecting heralded photons, and (c) is the concealed photon pattern when no trigger was used. (d) Propagation of nondiffracting correlated Airy photons over classical noise. When triggering of Stokes photons is used the self-bending of Airy photons is clearly visible. (e) Propagation of uncorrelated thermal Airy photons over classical noise. Without triggering the strong noise masks the Airy light. The overlaid theoretical curves indicate the peak (solid) and the half-maximum (dashed).

correlations to camouflage Airy-shaped photons in the presence of classical photon noise. The superimposed pattern of noise is introduced by Fourier transforming a weak laser beam by a pseudorandom distribution of disks imprinted on a phase-only SLM [28]. Figure 4(a) quantitatively demonstrates a crossover from the quantum to the classical regime where the noise overshadows the detected signal [28]. α/β represents the ratio of photons in the Airy, α, and in the classical noise pattern, β. Experimentally the ratio α/β is extracted by projecting the whole observed pattern to the predetermined Airy and noise profiles [28]. Figure 4(b) shows a pure Airy photon distribution even in the presence of classical noise. An observer without access to the trigger photons would detect noise-dominated patterns as the one in Fig. 4(c).

It must be noted that this quantum illumination behavior [31,32] is not unique to nondiffracting beams. The novelty here is the photon correlations are combined with the spreading resilience of spatial Airy photons. This resilience allowed us to observe propagation dynamics of Airy photons despite the noise background as illustrated in Figs. 4(d) and 4(e). The nondiffracting Airy photons can be revealed, by exploiting the correlations, after propagation as shown in Fig. 4(d). Even though, the speckled pattern was selected to have spatial features in the same scale as the Airy wave packets it diffracts dramatically faster. Figure 4(e) illustrates that without exploiting the correlations for so strong noise (more than a factor of 10 compared with the Airy shaped thermal light) the Airy pattern is unretrievable.

In this work, we have demonstrated for the first time spatiotemporal control of single photons in the form of quantum Airy wave packets, by merging quantum optics in cold atomic ensembles and nondiffracting spatial photonics. A mapping of the longitudinal modulation of a classical pumping beam has enabled us to sculpt the complex temporal wave function of the heralded photons, while their spatial degrees of freedom were controlled by subsequent transverse shaping. In addition, we have utilized the general concept of quantum illumination to demonstrate the interplay between temporal correlation and nondiffraction. For quantum communications nondiffraction [9] can extend the distance before noise starts dominating the optical signal and leads to larger than unity self-correlations, while it can be combined with entanglement self-healing and act as an excellent filter for long-distance optical communications [33,34]. Quantum imaging can benefit by combining an Airy point spread function as was utilized in [10,11] with photon postselection. As to other future directions, a second atomic ensemble or a crystal [35] with steep spectral features, as the ones encountered in electromagnetically induced transparency, can lead to the observation of spatiotemporal dynamics of single-photon bullets. Our work can shed light on important quests such as imaging and multimode information storage and encoding in the quantum regime [36,37]. Finally, generating abruptly autofocusing quantum wave packets [18,38] and nonparaxial single-photon bullets [4,15] is another exciting possibility [39,40].

[*] siviloglouga@sustech.edu.cn
[†] chenjf@sustech.edu.cn

[1] H.-H. Lu, E. M. Simmerman, P. Lougovski, A. M. Weiner, and J. M. Lukens, Phys. Rev. Lett. **125**, 120503 (2020).

[2] A. Valencia, A. Ceré, X. Shi, G. Molina-Terriza, and J. P. Torres, Phys. Rev. Lett. **99**, 243601 (2007).

[3] M. Kues, C. Reimer, P. Roztocki, L. R. Cortés, S. Sciara, B. Wetzel, Y. Zhang, A. Cino, S. T. Chu, B. E. Little, D. J. Moss, L. Caspani, J. Azaña, and R. Morandotti, Nature (London) **546**, 622 (2017).

[4] A. Pe'er, B. Dayan, A. A. Friesem, and Y. Silberberg, Phys. Rev. Lett. **94**, 073601 (2005).

[5] M. Erhard, M. Krenn, and A. Zeilinger, Nat. Rev. Phys. **2**, 365 (2020).

[6] H. Defienne, M. Reichert, and J. W. Fleischer, Phys. Rev. Lett. **121**, 233601 (2018).

[7] O. Jedrkiewicz, A. Gatti, E. Brambilla, and P. Di Trapani, Phys. Rev. Lett. **109**, 243901 (2012).

[8] J. Durnin, J. J. Miceli, and J. H. Eberly, Phys. Rev. Lett. **58**, 1499 (1987).

[9] G. A. Siviloglou, J. Broky, A. Dogariu, and D. N. Christodoulides, Phys. Rev. Lett. **99**, 213901 (2007).

[10] T. Vettenburg, H. I. C. Dalgarno, J. Nylk, C. Coll-Lladó, D. E. K. Ferrier, T. Čižmár, F. J. Gunn-Moore, and K. Dholakia, Nat. Methods **11**, 541 (2014).

[11] S. Jia, J. C. Vaughan, and X. Zhuang, Nat. Photonics **8**, 302 (2014).

[12] N. Voloch-Bloch, Y. Lereah, Y. Lilach, A. Gover, and A. Arie, Nature (London) **494**, 331 (2013).

[13] P. Polynkin, M. Kolesik, J. V. Moloney, G. A. Siviloglou, and D. N. Christodoulides, Science **324**, 229 (2009).

[14] D. Abdollahpour, S. Suntsov, D. G. Papazoglou, and S. Tzortzakis, Phys. Rev. Lett. **105**, 253901 (2010).

[15] A. Chong, W. H. Renninger, D. N. Christodoulides, and F. W. Wise, Nat. Photonics **4**, 103 (2010).

[16] D. Wei, Y. Yu, M. Cao, L. Zhang, F. Ye, W. Guo, S. Zhang, H. Gao, and F. Li, Opt. Lett. **39**, 4557 (2014).

[17] J. Baumgartl, M. Mazilu, and K. Dholakia, Nat. Photonics **2**, 675 (2008).

[18] P. Zhang, J. Prakash, Z. Zhang, M. S. Mills, N. K. Efremidis, D. N. Christodoulides, and Z. Chen, Opt. Lett. **36**, 2883 (2011).

[19] N. K. Efremidis, Z. Chen, M. Segev, and D. N. Christodoulides, Optica **6**, 686 (2019).

[20] S. Maruca, S. Kumar, Y. M. Sua, J.-Y. Chen, A. Shahverdi, and Y.-P. Huang, J. Phys. B **51**, 175501 (2018).

[21] O. Lib and Y. Bromberg, Opt. Lett. **45**, 1399 (2020).

[22] Z.-X. Li, Y.-P. Ruan, J. Tang, Y. Liu, J.-J. Liu, J.-S. Tang, H. Zhang, K.-Y. Xia, and Y.-Q. Lu, Opt. Express **29**, 40187 (2021).

[23] Y. Silberberg, Opt. Lett. **15**, 1282 (1990).

[24] L. Zhao, X. Guo, Y. Sun, Y. Su, M. M. T. Loy, and S. Du, Phys. Rev. Lett. **115**, 193601 (2015).

[25] L. Zhao, Y. Su, and S. Du, Phys. Rev. A **93**, 033815 (2016).

[26] P. Kolchin, C. Belthangady, S. Du, G. Y. Yin, and S. E. Harris, Phys. Rev. Lett. **101**, 103601 (2008).

[27] J. Broky, G. A. Siviloglou, A. Dogariu, and D. N. Christodoulides, Opt. Express **16**, 12880 (2008).

[28] See Supplemental Material at http://link.aps.org/supplemental/10.1103/PhysRevLett.132.143601 for more details on the experimental setup, the measurement protocols, the space-to-time mapping, and the spatial beam shaping.

[29] S. Zhang, J. F. Chen, C. Liu, M. M. T. Loy, G. K. L. Wong, and S. Du, Phys. Rev. Lett. **106**, 243602 (2011).

[30] B. M. Sparkes, J. Bernu, M. Hosseini, J. Geng, Q. Glorieux, P. A. Altin, P. K. Lam, N. P. Robins, and B. C. Buchler, New J. Phys. **15**, 085027 (2013).

[31] S. Lloyd, Science **321**, 1463 (2008).

[32] E. D. Lopaeva, I. Ruo Berchera, I. P. Degiovanni, S. Olivares, G. Brida, and M. Genovese, Phys. Rev. Lett. **110**, 153603 (2013).

[33] M. McLaren, T. Mhlanga, M. J. Padgett, F. S. Roux, and A. Forbes, Nat. Commun. **5**, 3248 (2014).

[34] X. Wang, J. Fu, S. Liu, Y. Wei, and J. Jing, Optica **9**, 663 (2022).

[35] L. Wang, Y.-H. Sun, R. Wang, X.-J. Zhang, Y. Chen, Z.-H. Kang, H.-H. Wang, and J.-Y. Gao, Opt. Express **27**, 6370 (2019).

[36] Y.-H. Ye, L. Zeng, M.-X. Dong, W.-H. Zhang, E.-Z. Li, D.-C. Li, G.-C. Guo, D.-S. Ding, and B.-S. Shi, Phys. Rev. Lett. **129**, 193601 (2022).

[37] C. Hang, Z. Bai, and G. Huang, Phys. Rev. A **90**, 023822 (2014).

[38] D. G. Papazoglou, N. K. Efremidis, D. N. Christodoulides, and S. Tzortzakis, Opt. Lett. **36**, 1842 (2011).

[39] I. Kaminer, R. Bekenstein, J. Nemirovsky, and M. Segev, Phys. Rev. Lett. **108**, 163901 (2012).

[40] P. Aleahmad, M.-A. Miri, M. S. Mills, I. Kaminer, M. Segev, and D. N. Christodoulides, Phys. Rev. Lett. **109**, 203902 (2012).